suspension and removal of the clay and silt matrix, and recycling of nutrients that would otherwise be trapped in the sediment. Hence gray whale feeding activity may be a significant factor contributing to the high benthic productivity of the Bering Shelf.

KIRK R. JOHNSON
Department of Geology, University of Pennsylvania, Philadelphia 19104
C. HANS NELSON
Branch of Pacific Marine Geology MS999, U.S. Geological Survey, Menlo Park, California 94025

References and Notes

1. At present 16,000 gray whales exist in the eastern Pacific (S. B. Reilly, paper presented at the Fifth Biennial Conference on the Biology of Marine Mammals, Boston, 1983).
2. M. Nerini, in *The Gray Whale*: Eschrichtius robustus, M. L. Jones *et al.*, Eds. (Academic Press, New York, in press).
3. D. W. Hood and J. A. Calder, Eds., *The Eastern Bering Sea Shelf: Oceanography and Resources* (Univ. of Washington Press, Seattle, 1981), vol. 2.
4. K. J. Frost and L. F. Lowry, in *ibid.*, pp. 825–836.
5. S. Moore and D. Ljungblad, in *The Gray Whale*: Eschrichtius robustus, M. L. Jones *et al.*, Eds. (Academic Press, New York, in press).
6. G. C. Ray and W. E. Schevill, *Mar. Fish. Rev.* **36**, 31 (1974).
7. J. S. Oliver, P. N. Slattery, M. A. Silberstein, E. F. O'Connor, *Can. J. Zool.*, in press.
8. J. Hudnall, paper presented at the Fourth Biennial Conference on the Biology of Marine Mammals, 1981.
9. The side-scan sonar is a planographic sea floor surveying device that generates sonographs analogous to aerial photographs of land areas. A description of side-scan sonar methods for evaluating gray whale feeding traces is given by K. R. Johnson, C. H. Nelson, and H. L. Mitchell [*U.S. Geol. Surv. Open-File Rep. 83-727* (1983)].
10. D. W. Rice and A. A. Wolman, *Am. Soc. Mammal. Spec. Publ. No. 3* (1971).
11. S. W. Stoker, in (*3*), pp. 1066–1091.
12. C. H. Nelson, R. W. Rowland, S. Stoker, B. R. Larsen, in (*3*), pp. 1265–1296.
13. A total of 221 stations were analyzed for amphipods. Sediment data for 684 stations were from G. R. Hess, B. R. Larsen, D. Klingman, and D. Moore [*Natl. Oceanic Atmos. Adm. Outer Cont. Shelf Environ. Assess. Program Annu. Rep. RU429* (1981)].
14. L. D. Consiglieri, H. W. Braham, L. L. Jones, *Natl. Oceanic Atmos. Adm. Outer Cont. Shelf Environ. Assess. Program Q. Rep. RU-68* (1980).
15. C. H. Nelson, *Geol. Mijnbouw* **61**, 37 (1982).
16. D. R. Thor and C. H. Nelson, in (*3*), pp. 279–291.
17. W. R. Dupré, *Geol. Mijnbouw* **61**, 63 (1982).
18. C. H. Nelson, D. R. Thor, M. W. Sandstrom, K. A. Kvenvolden, *Geol. Soc. Am. Bull.* **90**, 1144 (1980).
19. M. L. Larsen, C. H. Nelson, D. R. Thor, *Environ. Geol.* **3**, 47 (1979).
20. D. A. Cacchione and D. E. Drake, *J. Geophys. Res.* **87**, 1952 (1982).
21. D. H. Thomson, unpublished manuscript.
22. M. K. Nerini and J. S. Oliver [*Oecologia (Berlin)* **59**, 224 (1983)] and Thomson (*21*), working mainly in the nearshore areas southeast of Saint Lawrence Island, did not report any evidence of enlargement of whale feeding pits by current scouring. Pit enlargement is evidently a function of local current regime as well as season. The best examples of pit enlargement by current scouring are in the east-central Chirikov Basin.
23. We thank M. Nerini, J. Oliver, and D. Thomson for discussions concerning their research. This study was funded by the Bureau of Land Management through interagency agreement with the National Oceanographic and Atmospheric Administration as part of the Outer Continental Shelf Environmental Assessment Program.

28 February 1984; accepted 31 May 1984

Magnetic Cristobalite (?): A Possible New Magnetic Phase Produced by the Thermal Decomposition of Nontronite

Abstract. *Prolonged heat treatment (>1 hour) of nontronite (an iron-rich smectite clay) at 900° to 1000°C produces a phase with some unusual magnetic properties. This new phase has a Curie temperature of 200° to 220°C, extremely high remanent coercivities in excess of 800 milliteslas, and a room-temperature coercivity dependent on the magnitude of the applied field during previous thermomagnetic cycling from above 220°C. X-ray and magnetic analyses suggest that an iron-substituted cristobalite could be responsible, in part, for these observations. Formation of this magnetic cristobalite, however, may require topotactic growth from a smectite precursor.*

In an earlier study (*1*) we reported that thermal treatment of nontronite, an iron-rich smectite clay, could cause a dramatic increase in magnetic susceptibility and saturation magnetization (σ_s). For example, when nontronite is heated at 900°C in air for only 5 minutes, an x-ray amorphous aggregate is produced with a bulk σ_s of $\approx$6 to 10 A-m^2/kg (products possessing these properties display what is called type 1 behavior). Nontronite is believed to be an important component of the martian regolith (*2, 3*), and this heat-treated "meta-nontronite" has composition, color, and magnetic properties consistent with those recorded by the Viking spacecraft on Mars (*1, 4*). We report here further data on the magnetic properties of thermally treated nontronite, in particular, the discovery of (i) a new, magnetic phase with a Curie temperature (T_c) of 200° to 220°C and extremely high remanent coercivity (H_r >>800 mT), produced after prolonged heating at 900°C (behavior hereafter referred to as type 2), and (ii) the identification of the type 1 phase as a maghemite thermally stable to at least 1000°C. The formation of these two magnetic phases prompts considerations concerning the thermal transformations of iron-rich clay minerals, the stability and metastability of maghemite, and the possible applications of these phases as high-coercivity permanent magnet and magnetic tape materials.

A representative series of magnetization versus temperature (σ-T) curves are shown in Fig. 1 for samples of Manito nontronite (*5*) annealed at 900°C for periods ranging from 5 minutes to 193 hours. Two types of σ-T behavior are apparent in Fig. 1. As was also true for all other nontronite samples studied, after annealing times less than approximately 3 hours the σ-T curves are reversible ($\sigma_f/\sigma_i \approx 1$, where σ_f is the final magnetization after heating and σ_i is the initial magnetization before heating) and the magnetization decreases almost linearly with temperature (Fig. 1a). This σ-T behavior is another characteristic of the type 1 phase. Magnetic properties for samples exhibiting type 1 behavior also include (i) σ_s $\approx$6 to 10 A-m^2/kg, (ii) superparamagnetic behavior with an effective magnetic grain size of 70 to 150 Å, and (iii) no distinct Curie temperature (*1, 6*).

After samples have been heated for longer than 5 hours, the σ-T behavior begins to transform from type 1 to type 2, which becomes increasingly prominent after 13 hours. Type 2 behavior is characterized by (i) an increase in magnetization with temperature to $\approx$150°C (T_{max}), (ii) an apparent T_c of 200°C to 220°C, and (iii) a large increase in magnetization after heating ($\sigma_f/\sigma_i \approx 2$ to 5) (Fig. 1, c to f). As the annealing time increases beyond 13 hours, both T_{max} and σ_f/σ_i increase.

In addition to the irreversible σ-T behavior, type 2 samples are also unusual with respect to thermomagnetic cycling in an applied field. Initial σ-T curves exhibit the typical type 2 behavior (type 2a, Fig. 2a), but, if the applied field during cooling from above 220°C is >4 mT, then during subsequent thermomagnetic cycling the σ-T curves become almost reversible ($\sigma_f/\sigma_i \approx 1$ to 1.5) and the increase in magnetization during heating disappears (type 2b, Fig. 2b). If, however, the applied field during cooling from above 220°C is <4 mT, then the typical type 2a behavior returns during the next thermomagnetic cycle. The change from type 2a to type 2b is reversible, the behavior being determined by the magnitude of the applied field during cooling from above 200°C. The applied field also determines the values of T_{max} and σ_f/σ_i; an increase in the field causes both quantities to decrease.

Other magnetic properties for samples exhibiting type 2 behavior include the following: (i) a bulk σ_s of $\approx$3 to 5 A-m^2/kg; (ii) extremely high H_r, in excess of 800 mT; and (iii) high values of the ratio of saturation remanent magnetization (σ_r) to σ_s, $\approx$0.6 to 0.7.

In order to describe better the complex magnetic behavior produced by the thermal treatment of nontronite at 900°C, we have made the following simplifying generalizations. (i) The type 2 behavior is related to the phase responsible for T_c = 200° to 220°C. (ii) The applied field during the σ-T measurements (500 mT) is insufficient to saturate this phase fully at room temperature because of its high coercivity; saturation occurs as the temperature is raised, thereby producing the increase in magnetization with heating. (iii) After cooling from above 220°C, however, this phase is saturated at room temperature. (iv) Any other magnetic component present is presumed either to contribute negligibly to the magnetization at room temperature or can be saturated in 500 mT. (v) The difference in magnetization ($\Delta\sigma$) between σ_f and σ_i, therefore, must be proportional to the amount of the 220°C T_c phase. (vi) The magnetization at 600°C (σ_{600}) will be assumed to be proportional to the amount of hematite, but this hematite contribution is usually very small. The magnetization remaining at 300°C (σ_{300}) is therefore proportional to the amount of the magnetic phase responsible for type 1 behavior. These parameters are plotted in Fig. 3 as a function of annealing time. Initially, the type 1 component increases (σ_{300}), the hematite component remains constant, and the type 2 component ($\Delta\sigma$) is negligible. After ~3 hours, the type 2 component sharply increases, while the type 1 component drops precipitously. Thereafter, the amount of the type 2 component remains practically constant, but the type 1 component continues to decrease while the hematite component increases. These data suggest that the type 2 component (the 220°C T_c phase) is produced rapidly between 3 and 13 hours at 900°C at the expense of type 1; the only changes occurring after 13 hours is the continuous transformation of the remaining type 1 component into hematite.

X-ray analysis of the various thermally treated nontronite samples reveals that material heated for short periods is amorphous (*1*). In samples annealed for long times, the most abundant phase in addition to hematite has its strongest reflection corresponding to a *d*-spacing of ~4.1 Å, which we have identified as cristobalite (a high-temperature polymorph of quartz). Formation of cristobalite, in addition to a magnetic phase, by the thermal breakdown of nontronite has been reported (*7*). In our experiments, this cristobalite reflection is most intense after 100 hours at 900°C, or after 1 hour at 1000°C. When a sample annealed at 1000°C for 25 hours was treated with HF for 30 minutes, cristobalite (and any quartz present) was completely removed (as determined by x-ray analysis) and, surprisingly, both the type 2 and the type 1 phases were completely destroyed (as determined by σ-T analysis). The only magnetic phase remaining after HF treatment was hematite. A sample annealed at 1000°C for 1 hour was treated with HCl for 48 hours to remove iron oxides; this resulted in the partial removal of the type 1 and hematite components but there was little change in the type 2 component.

Results of magnetic and x-ray analyses for six other nontronites from different localities, each annealed at 1000°C for 1 hour, are summarized in Table 1. These samples can be grouped into four categories on the basis of their magnetic properties. Samples that have high values of $\Delta\sigma$ also have very strong cristobalite (111) reflections on x-ray. In contrast, those samples that have low values of $\Delta\sigma$ have very strong quartz (101) reflections

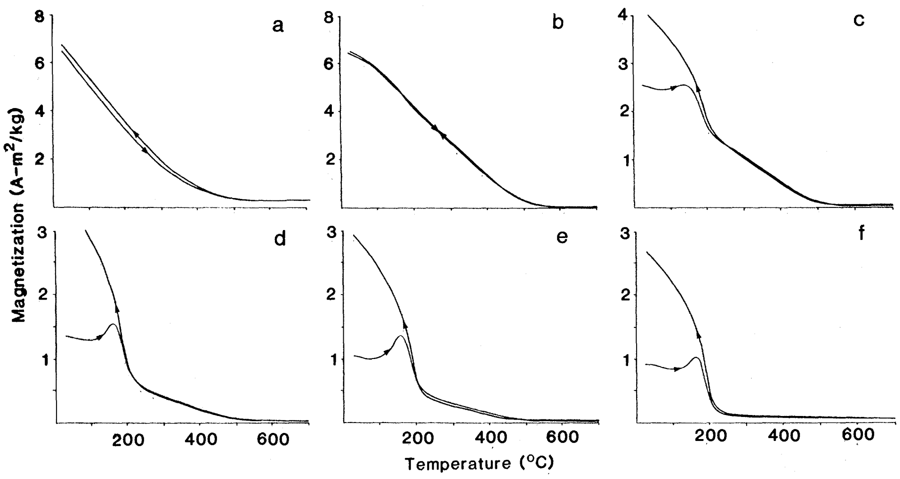

Fig. 1. The magnetization-temperature (σ-T) behavior for a series of samples from Manito, Washington, annealed at 900°C in air for various times: (a) 5 minutes; (b) 3 hours; (c) 13 hours; (d) 50 hours; (e) 100 hours; and (f) 193 hours. The applied field during the σ-T measurements is 500 mT.

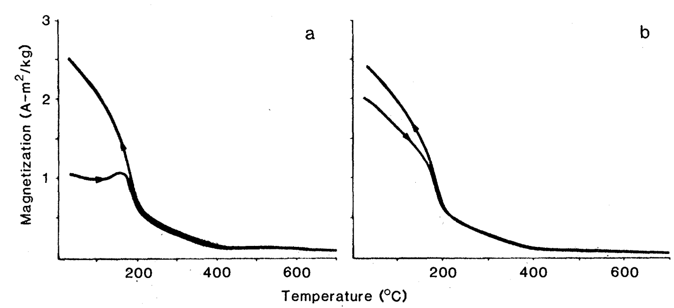

Fig. 2. The effect of an applied field (500 mT) during thermomagnetic cycling. The first heating (a) shows typical type 2a behavior. The second heating (b) shows type 2b behavior.

Table 1. Summary of the results of magnetic and x-ray analyses for nontronite thermally treated at 1000°C for 1 hour: ht, hematite (104); cris, cristobalite (111); qtz, quartz (101); sp, spinel (220); vs, very strong; s, strong; m, medium; w, weak; and vw, very weak. The nontronites are from the following sources: Manito, Washington (American Petroleum Institute sample H33b); Garfield, Washington (American Petroleum Institute sample H33a); Hagen, Germany, and Grant County, Washington (sample Swa-1; source, Clay Minerals Repository); Riverside, California (*2*); Hemet, California; and northeastern Alberta (*11*).

Sample	$\Delta\sigma$	σ_{300}	σ-T	Relative x-ray intensities			
				ht	cris	qtz	sp
Manito	1.80	0.150	2	vs	vs	w	m
Garfield	2.61	0.080	2	vs	vs	w	m
Hagen	0.393	0.183	2	m	vw	vs	vw
Swa-I	0.258	0.032	2	s	s	vs	vw
Riverside	0.19	2.18	1	s	w	m	m
Hemet	−0.46	4.36	1			vs	s
Northeastern Alberta	0.174	0.185	2	vs	w	vs	

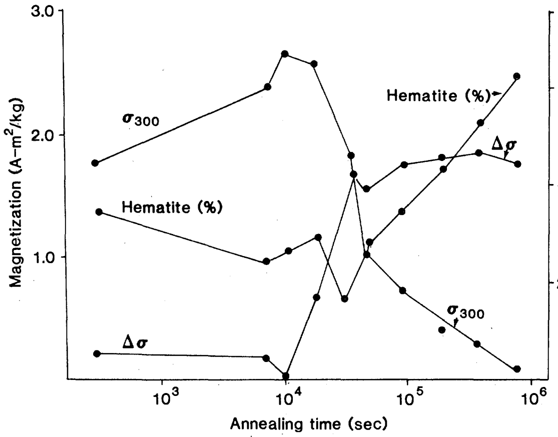

Fig. 3. The variation in the $\Delta\sigma$, σ_{300}, and percent hematite components as a function of annealing time for samples annealed at 900°C (Fig. 1).

on x-ray. Furthermore, the northeastern Alberta sample has a practically constant magnetization between 200° and 600°C and a large amount of hematite (23 percent), whereas all the other type 2 samples have a linear decrease in magnetization with temperature between 220° and 500°C and between 5 and 10 percent hematite. The (220) spinel reflection of varying intensity is present in x-ray for all the thermally treated nontronites in Table 1 except the northeastern Alberta nontronite. This peak is strongest in the Hemet and Riverside samples. Magnetic and detailed x-ray analysis of the thermally treated Hemet nontronite suggests that the type 1 behavior is due to this spinel phase, which is possibly maghemite, with a Curie temperature of 540°C (*8*).

The correlation between the presence of cristobalite and type 2 σ-T behavior is convincing. Although we do not have direct evidence for the existence of "magnetic cristobalite," it seems that the phase responsible for the 4.1-Å reflection is also responsible for type 2 magnetic behavior. A spinel phase, possible maghemite, is probably the type 1 component. Identification of the type 1 phase as a spinel is also consistent with the σ-T analysis (Fig. 3): prolonged annealing transforms this spinel to hematite. It is also clear from Table 1 that the crystallization of quartz rather than cristobalite inhibits the formation of the type 2 phase.

At this juncture we speculate that the type 2 phase is cristobalite, either iron-substituted or doped. Both the HF experiment and the negative correlation between the relative amounts ($\Delta\sigma$) of the type 2 phase produced and the appearance of quartz support this interpretation. If most of the SiO_2 in the original nontronite lattice is recrystallizing as quartz, then there will be less silica available to produce "iron-cristobalite." It is also intriguing that cristobalite is reported to undergo a displacive transition from the α-form (tetrahedral) to the β-form (cubic) between 180° and 280°C (*9*); this transition may be responsible for the apparent T_c at 220°C. On this hypothesis the α-form is (ferri?)magnetic, whereas the β-form is antiferromagnetic or paramagnetic. A mixture of αFe_2O_3 and colloidal SiO_2 in molar proportions equivalent to nontronite was annealed at 1550°C in the stability field of cristobalite (*9*) for 24 hours. X-ray analysis revealed only cristobalite, Fe_3O_4, and αFe_2O_3, but magnetic measurements showed that no type 2 phase was produced. Possibly the formation of magnetic cristobalite at 900° to 1000°C requires topotactic growth from a smectite precursor.

Although we do not yet have an adequate explanation for the field cooling experiments (Fig. 2), they do suggest that their ultimate cause may be exchange anisotropy (*10*). This exchange anisotropy could be produced by the interaction between the type 1 and type 2 phases or by the interactions between ferromagnetic and antiferromagnetic regions produced by compositional fluctuations within the type 2 phase alone. Further research is needed to resolve this uncertainty.

BRUCE M. MOSKOWITZ
ROBERT B. HARGRAVES

Department of Geological and Geophysical Sciences, Princeton University, Princeton, New Jersey 08544

References and Notes

1. B. M. Moskowitz and R. B. Hargraves, *J. Geophys. Res.* **87**, 10 (1982).
2. P. Toulmin III *et al.*, *ibid.* **82**, 4625 (1977).
3. C. Allen, J. L. Gooding, M. Jercinsvic, K. Keil, *Icarus* **45**, 347 (1981); A. Banin and L. Margulies, *Nature (London)* **305**, 523 (1983).
4. R. B. Hargraves, D. W. Collinson, R. E. Arvidson, C. R. Spitzer, *J. Geophys. Res.* **82**, 4547 (1977); R. B. Hargraves, D. W. Collinson, R. E. Arvidson, P. M. Cates, *ibid.* **84**, 8379 (1979).
5. P. F. Kerr *et al.*, *Am. Pet. Inst. Res. Proj.* **49**, (Report No. 7) (1951).
6. B. M. Moskowitz and R. B. Hargraves, *Eos* **63**, 310 (1982).
7. R. J. D. Mackenzie and E. D. Rogers [*Thermochim. Acta* **18**, 177 (1977)] claimed that maghemite was produced by the thermal decomposition of their nontronite samples.
8. If the type 1 phase is maghemite, then the maghemite exhibits very high stability with heating. In (*7*) it was suggested that this was due to the presence of silicon in the maghemite structure.
9. W. A. Deer, R. A. Howie, J. Zussman, *Rock-Forming Minerals* (Wiley, New York, 1963), vol. 4, p. 343.
10. W. H. Meiklejohn and C. P. Bean, *Phys. Rev.* **105**, 904 (1957).
11. W. Petruk, D. M. Eirrell, E. E. Lavier, R. J. Tremblayu, P. G. Manning, *Can. Mineral* **15**, 14 (1977).

12. We thank C. Lawson and S. K. Banerjee for helpful discussions and critical comments. We thank R. Stallard, F. B. Van Houten, and A. K. Baird who contributed samples of nontronite. This work was supported by NASA grant NAGW-372.

27 February 1984; accepted 12 June 1984

Remote Acoustic Imaging of the Plume from a Submarine Spring in an Arctic Fjord

Abstract. *Acoustic backscatter observations at 200 kilohertz were made of the buoyant plume from a submarine spring at a depth of 47 meters in Cambridge Fiord, Baffin Island. Vertical velocities of up to 37 centimeters per second are inferred from the ascent rates of discrete scattering structures in the plume.*

A plume of brackish water has been observed rising from a submarine spring at a depth of 47 m on the prodelta at the head of Cambridge Fiord, Baffin Island. The observations were made from a 10-m launch during September in 1982 and 1983, and include 200-kHz acoustic backscatter images of the plume and conductivity-temperature-depth (CTD) and vertical velocity profiles (*1*). These results appear to be novel and to have useful implications for the monitoring of buoyant plumes in the marine environment in general.

The discharge of ground water through the sea floor has only recently become a focus for research, and most known points of outflow occur in water shallow enough for the plume to rise to the surface (*2*). Evidence has been presented, however, suggesting that such discharge occurs at depths as great as 500 m on the Florida continental slope (*3*) and that ground water seepage on the conti-